

Estimating the gravitational wave background anisotropy: a Bayesian approach boosted by cross-correlation angular power spectrum

Chi Tian,¹ Ran Ding,^{1,*} and Xiao-Xiao Kou^{2,†}

¹*School of Physics and Optoelectronics Engineering,
Anhui University, 111 Jiulong Road, Hefei, Anhui 230601, China*

²*School of Physics and Astronomy, University of Minnesota, Minneapolis, MN 55455, USA*

We introduce a new method designed for Bayesian inference of the angular power spectrum of the Gravitational Wave Background (GWB) anisotropy. This scheme works with time-series data and can optionally incorporate the cross-correlations between the GWB anisotropy and other cosmological tracers, enhancing the significance of Bayesian inference. We employ the realistic LISA response and noise model to demonstrate the validity of this approach. The findings indicate that, without considering any cross-correlations, the 4-year LISA data is insufficient to achieve a significant detection of multipoles. However, if the anisotropies in the GWB are strongly correlated with the Cosmic Microwave Background (CMB), the 4-year data can provide unbiased estimates of the quadrupole moment ($\ell = 2$). This reconstruction process is generic and not restricted to any specific detector, offering a new framework for extracting anisotropies in the GWB data from various current and future gravitational wave observatories.

Introduction — Our ability to detect gravitational waves (GWs) will undoubtedly reach an unprecedented level in the next decade, with detection ranges spanning from nanohertz to several hundred hertz and significantly enhanced precision. This substantial advancement is likely to help us fully decipher a new background signal in the Universe — the gravitational wave background (GWB), whose preliminary clues have been revealed by recent Pulsar Timing Array experiments [1–4]. This diffused GW signal, resulting from superpositions of numerous unresolved sources, can be classified into two categories: the astrophysical gravitational wave background (AGWB) and the cosmological gravitational wave background (CGWB). The former results from superpositions of unresolved galactic and extra-galactic sources, mostly related to the dynamics of compact objects [5–10]. The latter, originating from early Universe processes, is closely related to new physics, such as inflation, reheating/preheating, primordial black holes, topological defects, or cosmological first-order phase transitions [11–15].

Similar to the CMB and other cosmological probes, the GWB also carries anisotropies, which can originate from either source distributions or propagation processes. Anisotropies arising from sources include those generated by inhomogeneous distributions of compact objects [16], in the case of the AGWB, or those resulting from large scale perturbations introduced by domain walls in the early universe [17], as in the CGWB. On the other hand, the propagation process may lead to anisotropies due to various gravitational effects, analogous to the CMB photons [18]. Considerable efforts have been made in recent years to model the angular power spectrum of the GWB anisotropy [19–38] and to assess its detectability

in the operating and proposed GW observations [39–45]. These investigations have primarily focused on signal-to-noise ratio (SNR) estimations or sky map reconstructions [46–53]. However, to facilitate a comparison with physical models, a Bayesian framework for extracting angular spectra directly from time-series data is necessary. Moreover, as predicted by many theoretical studies [24, 41, 54, 55], regardless of their astrophysical or cosmological origins, the anisotropies in the GWB generally exhibit significant cross-correlations with other existing cosmological tracers, such as the CMB, the CMB lensing, or large-scale structures. The detection sensitivity to the anisotropies would undoubtedly benefit from these potential cross-correlations, as suggested by [39, 41, 42], through estimating the enhanced SNR. Nevertheless, a consistent methodology for integrating these cross-correlations into the data-analysis framework, facilitating the extraction of the angular power spectrum of the GWB anisotropy, has not been established.

In this letter, we focus on a novel data analysis scheme designed to extract anisotropies in the form of the angular power spectrum directly from time-series data of GW detectors. This framework optionally accounts for the potential cross-correlations between the anisotropic GWB and other cosmological tracers. We demonstrate the validity of this approach by applying it to LISA [56, 57] mock data and discuss its broader applications for future GW observations.

Anisotropic GWB intensity and time-series data — Assuming the GWs to be Gaussian, stationary and unpolarized, the metric perturbation $h_p(f, \hat{\mathbf{n}})$ in Fourier space is characterized by its quadratic expectation values as

$$\langle h_p(f, \hat{\mathbf{n}}) h_{p'}^*(f', \hat{\mathbf{n}}') \rangle \equiv \delta(f - f') \frac{\delta^2(\hat{\mathbf{n}}, \hat{\mathbf{n}}')}{4\pi} W_{pp'}(f, \hat{\mathbf{n}}), \quad (1)$$

where $p = \{+, \times\}$ labels the polarization states, $\hat{\mathbf{n}}$ is the direction of propagation in the sky and the matrix

* Corresponding author: dingran@mail.nankai.edu.cn

† Corresponding author: kou00016@umn.edu

W is related to the gravitational Stokes parameters Q , U , and V . Under the unpolarized condition, $Q = U = V = 0$, one has $W_{+, \times}(f, \hat{\mathbf{n}}) = I(f, \hat{\mathbf{n}})$, where $I(f, \hat{\mathbf{n}})$ represents the GW intensity.

On the other hand, when considering the GWB, it's a common practice to quantifying it through the fractional energy density Ω_{GW} , whose spectrum can be separated into a background part (monopole) and a linear fluctuation. It can be proven [49, 58] the relationship between the anisotropic GW intensity and the fractional energy density, using the spherical harmonic coefficients, can be expressed by

$$I_{00}(f) \equiv \frac{3H_0^2 \bar{\Omega}_{\text{GW}}(f)}{4\pi^2 f^3}, \quad (2)$$

and

$$\begin{aligned} I_{\ell m}(f) &= \frac{3H_0^2 \bar{\Omega}_{\text{GW}}(f)}{4\pi^2 \sqrt{4\pi} f^3} \left(4 - \frac{\partial \ln \bar{\Omega}_{\text{GW}}(f)}{\partial \ln f} \right) a_{\ell m}^{\text{GW}} \\ &\equiv K_f a_{\ell m}^{\text{GW}}, \end{aligned} \quad (3)$$

where we have assumed that K_f has encapsulated all the frequency dependencies, leaving $a_{\ell m}^{\text{GW}}$ s frequency-independent, which is exactly true when Ω_{GW} has a power-law spectrum. Our aim is to extract the power spectrum of $a_{\ell m}^{\text{GW}}$, denoted as C_ℓ^{GW} , from the time-series data.

The time-series data of a GW detector A, denoted as $d_t^A(f)$, is obtained by applying Fourier transforms to the signal over a specific time segment T_{seg} , at given time t , resulting in

$$d_t^A(f) = \int d^2\Omega_{\hat{\mathbf{n}}} \sum_p R_{t,p}^A(f, \hat{\mathbf{n}}) h_p(f, \hat{\mathbf{n}}) + n_{t,f}^A, \quad (4)$$

where $R_{t,p}^A(f, \hat{\mathbf{n}})$ and $n_{t,f}^A$ are the response function and noise for the detector A. $d_t^A(f)$ has a zero mean, and its ensemble average, evaluated at equal time and frequency (and is otherwise zero), can be estimated by

$$\begin{aligned} \langle D_{t,f}^{AB} \rangle &\equiv \frac{2}{T_{\text{seg}}} \langle d_t^A(f) d_t^{B*}(f) \rangle \\ &= \sum_{\ell=0}^{\infty} \sum_{m=-\ell}^{\ell} \gamma_{\ell m}^{AB}(t, f) I_{\ell m}(f) + N_{t,f}^{AB}, \end{aligned} \quad (5)$$

where $N_{t,f}^{AB} \equiv (2/T_{\text{seg}}) \langle n_{t,f}^A n_{t,f}^{B*} \rangle$ is the noise power spectral density (PSD) for the detector pair AB, and $\gamma_{\ell m}^{AB}(t, f)$ are spherical harmonic coefficients of the response function $\gamma_{t,f}^{AB}(\hat{\mathbf{n}})$ for this detector pair, defined by

$$\gamma_{t,f}^{AB}(\hat{\mathbf{n}}) = \Delta\Omega \sum_p R_{t,p}^A(f, \hat{\mathbf{n}}) R_{t,p}^{B*}(f, \hat{\mathbf{n}}). \quad (6)$$

The covariance of $D_{t,f}^{AB}$, at the same time and frequency, can be written as

$$\begin{aligned} C_{t,f}^{ABCD} &\equiv \langle D_{t,f}^{AB} D_{t,f}^{CD*} \rangle \\ &\approx (\gamma_{00}^{AC}(t, f) I_{00}(f) + N_{t,f}^{AC}) (\gamma_{00}^{DB}(t, f) I_{00}(f) + N_{t,f}^{DB}), \end{aligned} \quad (7)$$

where we have dropped contributions from multipoles in the approximation, which are subdominant.

Likelihood with cross-correlations — Our aim is to perform Bayesian estimations on the angular power spectrum of the GWB anisotropy using the time-series dataset $D_{\{t,f\}}^{\{AB\}}$. For this purpose, a practical likelihood function is necessary. When a set of $I_{\{\ell m\},f}$ is given, the likelihood for $D_{t,f}^{\{AB\}}$, which represents data for various detector's combinations at a specific time and frequency, can be simply written as

$$\begin{aligned} \mathcal{L}(D_{t,f} | I_{\{\ell m\},f}) &= \prod_{AB,CD} \frac{1}{|\pi C_{t,f}^{ABCD}|} \times \\ &\exp \left\{ - \left(D_{t,f}^{AB} - \langle D_{t,f}^{AB} \rangle \right)^\dagger (C_{t,f}^{ABCD})^{-1} \left(D_{t,f}^{CD} - \langle D_{t,f}^{CD} \rangle \right) \right\}. \end{aligned} \quad (8)$$

However, for a given angular power spectrum $C_{\{\ell\}}^{\text{GW}}$, there are in principle an infinite number of realizations in terms of $I_{\{\ell m\}}$, preventing us from writing down a likelihood function that directly links the time-series data with the model predicted $C_{\{\ell\}}^{\text{GW}}$. Therefore, we must remain agnostic regarding specific realizations.

In addition, the GWB anisotropy may be correlated with other cosmological tracers. Assuming that the GWB is cross-correlated with a known cosmological tracer Y, it is acknowledged that maps of the GWB together with the tracer Y can be represented by multivariate Gaussian variables with the covariance specified by their auto angular spectra C_ℓ^{GW} , C_ℓ^{Y} and the cross spectrum $C_\ell^{\text{GW} \times \text{Y}}$. Consequently, the conditional probability for the GWB can be derived with the knowledge of Y, whose measured spherical harmonics coefficients are $a_{\{\ell m\}}^{\text{Y}}$ with negligible uncertainties compared to the GWB measurements. It can be proven that for a given condition characterized by the combination of $(a_{\{\ell m\}}^{\text{Y}}, C_{\{\ell\}}^{\text{GW}}, C_{\{\ell\}}^{\text{GW} \times \text{Y}})$, the conditional distribution of $I_{\{\ell m\}}$ at a given frequency, denoted as $\mathcal{L}(I_{\{\ell m\},f} | \text{GW} \times \text{Y})$, obeys

$$\begin{aligned} \mathcal{L}(I_{\{\ell m\},f} | \text{GW} \times \text{Y}) &= \prod_{\substack{\ell m \\ \ell \geq 1}} \frac{1}{\pi C_\ell^{\text{GW} | \text{Y}}} \exp \left(- \frac{|I_{\ell m, f} - K_f \mu_{\ell m}^{\text{GW} | \text{Y}}|^2}{K_f^2 C_\ell^{\text{GW} | \text{Y}}} \right), \end{aligned} \quad (9)$$

where we have defined the mean and the auto-correlation of this GWB anisotropy as

$$\mu_{\ell m}^{\text{GW} | \text{Y}} \equiv \frac{C_\ell^{\text{GW} \times \text{Y}}}{C_\ell^{\text{Y}}} a_{\ell m}^{\text{Y}}, \quad (10)$$

$$\begin{aligned} C_\ell^{\text{GW} | \text{Y}} &\equiv C_\ell^{\text{GW}} - \frac{(C_\ell^{\text{GW} \times \text{Y}})^2}{C_\ell^{\text{Y}}} \\ &= C_\ell^{\text{GW}} \left[1 - (r^{\text{GW} \times \text{Y}})^2 \right], \end{aligned} \quad (11)$$

for $\ell \geq 1$, and the relative cross-correlation $r^{\text{GW} \times \text{Y}}$ is defined by $r^{\text{GW} \times \text{Y}} \equiv C_\ell^{\text{GW} \times \text{Y}} / \sqrt{C_\ell^{\text{GW}} C_\ell^{\text{Y}}}$. Note that

since the intensity monopole I_{00} is related to the GW fractional energy, as in eq. (2), the product in eq. (9) does not include the $\ell = 0$ term.

To finally derive the likelihood for the entire data set $D_{\{t,f\}}$ while remaining agnostic to the specific realization, we marginalize over all $I_{\ell m}$ s and sum over contributions from all time and frequency bins by computing

$$\mathcal{L}(D_{\{t,f\}} | \text{GW} \times \text{Y}) = \prod_{t,f} \int \mathcal{D}I_{\ell m,f} \mathcal{L}(D_{t,f} | I_{\{\ell m\},f}) \mathcal{L}(I_{\{\ell m\},f} | \text{GW} \times \text{Y}). \quad (12)$$

Then, by plugging in the expression from eqs. (5) and (7) to (9), and after some algebra, we finally arrive at a very compact form of the likelihood function:

$$\mathcal{L}(D_{\{t,f\}} | \text{GW} \times \text{Y}) \propto \prod_{t,f} |\pi C_{ab}|^{-1} \exp(-J_a^\dagger C_{ab}^{-1} J_b), \quad (13)$$

$$C_{ab} = C_{ab}^D + \Gamma_{a\mu} C_{\mu\nu}^I \Gamma_{\nu b}^*, \quad (14)$$

$$J_a = D_a - \Gamma_{a\mu} \bar{Z}_\mu - N_a. \quad (15)$$

Note that all quantities in eq. (13) depend on the time and frequencies, and for simplicity, we have used Latin letters, such as a and b , to compress the detector combinations, such as AB , into a single index. Additionally, we use Greek letters μ, ν , etc., to denote combinations of ℓm s. Following this convention, we have also defined $\Gamma_{a\mu} \equiv \gamma_{\{\ell m\}}^{\{AB\}}$, and $\bar{Z}_\mu \equiv \mu_{\ell m}^{\text{GW}|\text{Y}}$ for $\ell, \mu \geq 1$ and $\bar{Z}_0 \equiv I_{00}$ (see eq. (2)) for $\ell, \mu = 0$. We also denote C_{ab}^D to be the covariance described in eq. (7) and $C_{\mu\nu}^I$ to be a diagonal matrix expanded from $C_\ell^{\text{GW}|\text{Y}}$ by

$$C_{\mu\nu}^I \equiv K_f^2 \text{diag} \left(\underbrace{0, C_1^{\text{GW}|\text{Y}}, \dots, C_{\ell_{\max}}^{\text{GW}|\text{Y}}}_{(\ell_{\max}+1)^2 \text{ terms}}, \underbrace{C_{\ell_{\max}}^{\text{GW}|\text{Y}}, \dots, C_{\ell_{\max}}^{\text{GW}|\text{Y}}}_{(2\ell_{\max}+1) \text{ terms}} \right). \quad (16)$$

Eqs eqs. (13) to (15) are the main results of this letter. It is also important to know that this likelihood is generic, being applicable to models that are not considering any cross-correlations. In such case, one has $C_\ell^{\text{GW} \times \text{Y}} = 0$, and the mean and the covariance of harmonic coefficients are reduced to $\bar{Z}_\mu = K_f \mu_{\ell m}^{\text{GW}|\text{Y}} = 0$ for $\mu \geq 1$ and $C_\ell^{\text{GW}|\text{Y}} = C_\ell^{\text{GW}}$, producing a likelihood function of GW angular power spectrum without considering any cross-correlations, similarly as the results in [52, 59].

Bayesian inference of LISA mock data — For demonstration purposes, we inject anisotropic GWB signals to LISA and attempt to estimate the injected anisotropic level. The injected signal has a power-law spectrum $\Omega_{\text{GW}}(f) = A(f/f_{\text{ref}})^\alpha$, where we have

chosen $A = 10^{-10}$, $f_{\text{ref}} = 10^{-3}$ Hz and $\alpha = 1$, as depicted in the upper panel of Fig. 1. It is a relatively strong signal compared to the LISA sensitivity and the predicted spectrum of compact binaries [5–9]. Therefore, this mock signal can be considered as a GWB from new physics, which may arise from first order phase transitions or inflationary models (see [60, 61] for comprehensive reviews).

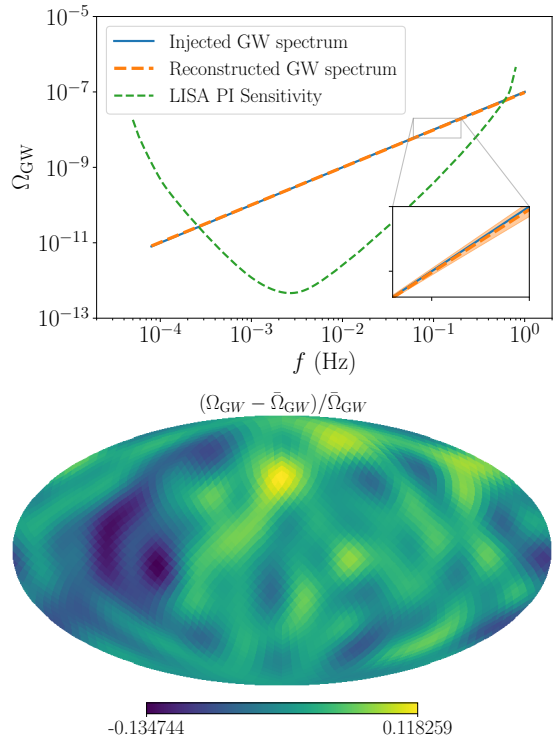


FIG. 1. **Upper Panel:** Injected and reconstructed GWB spectrum. The 1σ uncertainty is represented by the nearly invisible shaded region; **Lower Panel:** The sky map of the injected GWB, with the angular power spectrum satisfying $\log_{10} \tilde{C}_\ell^{\text{GW}} = -2.4$. Map pixels' locations are following the HealPix[62] convention with $N_{\text{side}} = 16$.

The anisotropies in the signal are generated based on a scale invariant angular spectrum of $a_{\ell m}^{\text{GW}}$ s, implying that $\tilde{C}_\ell^{\text{GW}} \equiv \ell(\ell+1)C_\ell^{\text{GW}} = \text{Const}$. This is a typical prediction of many cosmological models at low ℓ s. [24, 41, 54]. Our primary task is to estimate the $\tilde{C}_\ell^{\text{GW}}$ from the mock data. To this end, we generate a time-series data set $\{d_A^t(f)\}$ following the covariance given by eq. (5) in the frequency range $f \sim [0.0001, 0.2]$ Hz with $\Delta f = 10^{-6}$ Hz. This frequency spacing corresponds to an observation segment $T_{\text{seg}} \sim 11$ days, generating 25 different observation segments in a year, corresponding to a 75% observation efficiency. Each segment has a different antenna pattern due to the satellite array's varying orientations over a year. We compute the LISA response and the noise PSD using the public code `schNe11` [40], which estimates the LISA time-dependent response function based on spacecraft

positions over time, as derived in [63], while assuming a time-independent noise [58].

Once the fiducial data is injected, we first attempt to recover the monopole data (see Fig. 1). This can be simply done by employing eq. (13) and setting $C_{\mu\nu}^I$ to zero. The nearly invisible shaded region indicates that the uncertainties in the reconstructed monopole signals are negligible. The small uncertainties suggest that the contributions from the multipoles in the likelihood can be safely ignored when inferring the monopole spectrum. We therefore fix the reconstructed monopole parameters during the subsequent inferences of the angular power spectrum.

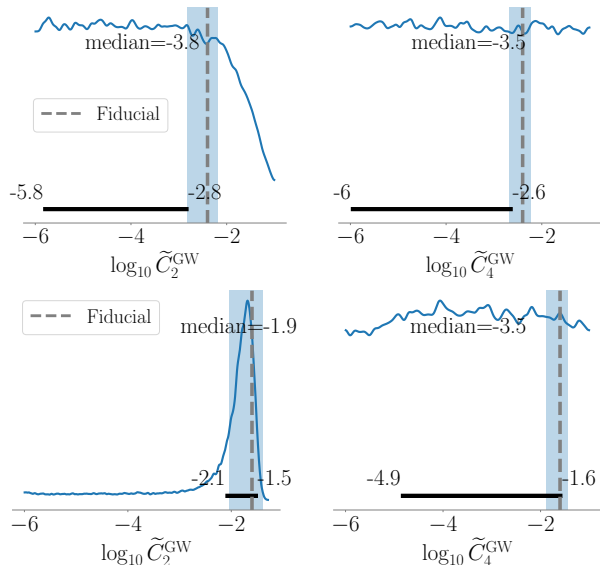


FIG. 2. **Upper Panel:** Reconstructed multipoles \tilde{C}_2^{GW} and \tilde{C}_4^{GW} based on the LISA 4-year data. Fiducial $\log_{10} \tilde{C}_\ell^{\text{GW}} = -2.4$. **Lower Panel:** Reconstructed multipoles based on the LISA 80-year data. Fiducial $\log_{10} \tilde{C}_\ell^{\text{GW}} = -1.6$. The black bars on the bottom mark the 1σ region, and the shaded regions represent the cosmic variance.

We then employ the full likelihood in eq. (13) to estimate the magnitude of the lowest several multipoles. To avoid potential numerical instabilities in the matrix inverses, in our calculation, we compute the matrix inverse by expanding the term $\Gamma_{a\mu} C_{\mu\nu}^I \Gamma_{\nu b}^*$ in eq. (14) to the 2nd order. The resulting posteriors are presented in Fig. 2. It is apparent that the LISA 4-year mission lacks sufficient sensitivity to recover the magnitude of multipoles in the GWB. This finding is consistent with other studies [39, 42, 45] based on the analysis of the SNR. Note that we only present the results for even multipoles, as the even parity of the LISA antenna pattern results in a weak SNR in the odd multipoles. We also find that unrealistically extending the LISA mission to 80 years and increasing the anisotropic level to $\log_{10} \tilde{C}_\ell^{\text{GW}} = -1.6$ will result in a posterior for the quadrupole moment \tilde{C}_2^{GW} whose 1σ region is comparable

to the cosmic variance $\sigma_{\tilde{C}_\ell^{\text{GW}}} = \sqrt{2/(2\ell+1)} \tilde{C}_\ell^{\text{GW}}$ [64], thereby suggesting the validity of our scheme.

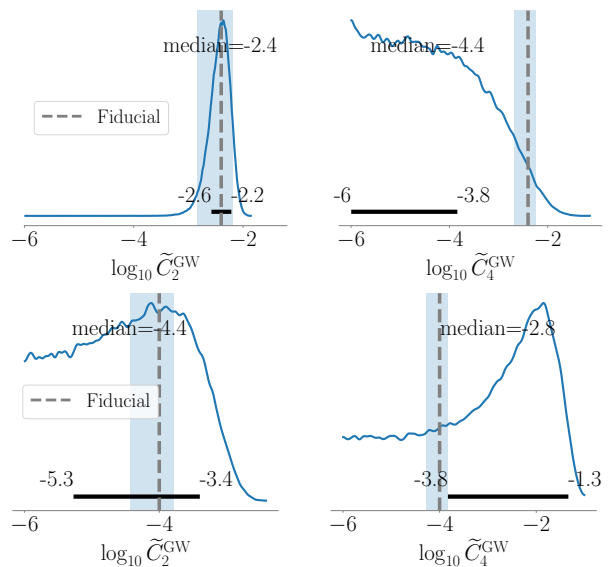


FIG. 3. Reconstructed multipoles based on the LISA 4-year data, assuming a perfect cross-correlations between the GWB and the CMB. **Upper Panel:** The fiducial $\log_{10} \tilde{C}_\ell^{\text{GW}} = -2.4$. **Lower Panel:** The fiducial $\log_{10} \tilde{C}_\ell^{\text{GW}} = -4$. The black bars on the bottom mark the 1σ region, and the shaded regions represent the cosmic variance.

Depending on the sources, the anisotropies in the GWB generally show different levels of cross-correlations with diverse cosmological tracers. For the CGWB, current models suggest that it has a strong correlation with the CMB or the CMB lensing [24, 41, 54]. To explore the most optimistic constraints on the LISA detectability based on known cross-correlations, we consider an ideal scenario in which the GWB is perfectly correlated with the CMB. Under this assumption, we inject a GWB fully correlated with the CMB by setting $r^{\text{GW}\times\text{CMB}} = 1$, subsequently employing this scheme to infer the magnitude of the lowest several multipoles in the GWB. Our findings indicate that the LISA 4-year data is able to provide unbiased estimations of quadrupole \tilde{C}_2^{GW} when $\log_{10} \tilde{C}_\ell^{\text{GW}} = -2.4$, as suggested by the upper panel in Fig. 3, confirming the validity of our scheme. As the bottom panel in Fig. 3 implies, this reconstruction works until approximately $\log_{10} \tilde{C}_\ell^{\text{GW}} \simeq -4$.

We have also simulated a GWB map based on a smaller relative correlation with the CMB, specifically $r^{\text{GW}\times\text{CMB}} = 0.85$ with $\log_{10} \tilde{C}_\ell^{\text{GW}} = -2.4$. By employing the likelihood function given in eq. (13) and taking $r^{\text{GW}\times\text{CMB}}$ as a new parameter, we plot $r^{\text{GW}\times\text{CMB}}$ vs. \tilde{C}_2^{GW} contour in Fig. 4. The results indicate that, even under the condition of a weaker correlation, our scheme remains effective in inferring quadrupole \tilde{C}_2^{GW} : the fiducial value can still be recovered within a 1σ confident level.

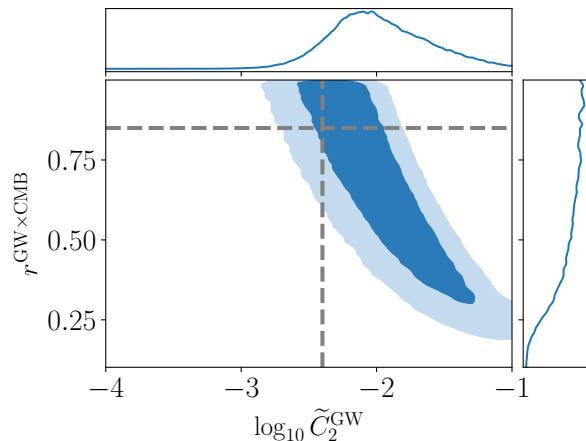


FIG. 4. Contour and posterior plots of the quadrupole \tilde{C}_2^{GW} and relative cross-correlation. The fiducial $r^{\text{GW} \times \text{CMB}} = 0.85$ and $\log_{10} \tilde{C}_2^{\text{GW}} = -2.4$. The grey dashed lines denote the fiducial values. Shaded regions represent the 1σ and 2σ range.

Discussions — In this study, we introduce a novel scheme for performing Bayesian inference on time-series data associated with the stochastic gravitational wave background. Utilizing a new analytical likelihood function, this approach directly connects the time-series data to the angular power spectrum, with the capability to incorporate the cross-correlations between the GWB anisotropy and any cosmological tracers. As a crucial feature of the GWB anisotropy, these cross-correlations, predicted by various physical models, can significantly enhance the reconstruction capability of our framework.

We employ forecasted LISA response and noise to demonstrate the validity of this approach. Our findings

indicate that, without considering any cross-correlations, the noise level in the 4-year LISA data prevents us from constructing reliable Bayesian inference on multipoles unless the LISA mission is unrealistically extended to 80 years. However, if the anisotropies in the GWB are strongly correlated with another cosmological tracer, such as the CMB, the 4-year LISA data can provide unbiased estimates of the quadrupole moment.

We emphasize that this scheme is designed generically for arrays of GW detectors. Our work, therefore, paves the way for detailed studies of the detectabilities of anisotropies in future ground-based and space-based GW observations, such as TianQin [65], Taiji [66, 67], DECIGO [68], BBO [66, 67], ET [69], and their possible joint searches [70–72]. The exploration of open questions, such as how various GWB source models are constrained from the GWB anisotropy, or how to differentiate between astrophysical and cosmological sources based on the anisotropies, might benefit from this new scheme. However, the focus of this letter is on the success of the method rather than the detectability for a specific detector or constraining GWB source models; we will therefore leave the detailed analysis on these topics for future studies.

Acknowledgments — Authors would like to thank Erik Floden, Vuk Mandic, Leo Tsukada and Gang Wang. R.D. is supported in part by the National Key R&D Program of China (No. 2021YFC2203100). C.T. is supported by the National Natural Science Foundation of China (Grants No. 12405048) and the Natural Science Foundation of Anhui Province (Grants No. 2308085QA34). The authors acknowledge the High-performance Computing Platform of Anhui University for providing computing resources.

-
- [1] Gabriella Agazie *et al.* (NANOGrav), “The NANOGrav 15 yr Data Set: Evidence for a Gravitational-wave Background,” *Astrophys. J. Lett.* **951**, L8 (2023), [arXiv:2306.16213 \[astro-ph.HE\]](#).
- [2] Heng Xu *et al.*, “Searching for the Nano-Hertz Stochastic Gravitational Wave Background with the Chinese Pulsar Timing Array Data Release I,” *Res. Astron. Astrophys.* **23**, 075024 (2023), [arXiv:2306.16216 \[astro-ph.HE\]](#).
- [3] J. Antoniadis *et al.* (EPTA), “The second data release from the European Pulsar Timing Array III. Search for gravitational wave signals,” (2023), [arXiv:2306.16214 \[astro-ph.HE\]](#).
- [4] Daniel J. Reardon *et al.*, “Search for an Isotropic Gravitational-wave Background with the Parkes Pulsar Timing Array,” *Astrophys. J. Lett.* **951**, L6 (2023), [arXiv:2306.16215 \[astro-ph.HE\]](#).
- [5] Valeria Ferrari, Sabino Matarrese, and Raffaella Schneider, “Stochastic background of gravitational waves generated by a cosmological population of young, rapidly rotating neutron stars,” *Mon. Not. Roy. Astron. Soc.* **303**, 258 (1999), [arXiv:astro-ph/9806357](#).
- [6] Valeria Ferrari, Sabino Matarrese, and Raffaella Schneider, “Gravitational wave background from a cosmological population of core collapse supernovae,” *Mon. Not. Roy. Astron. Soc.* **303**, 247 (1999), [arXiv:astro-ph/9804259](#).
- [7] Raffaella Schneider, Valeria Ferrari, Sabino Matarrese, and Simon F. Portegies Zwart, “Gravitational waves from cosmological compact binaries,” *Mon. Not. Roy. Astron. Soc.* **324**, 797 (2001), [arXiv:astro-ph/0002055](#).
- [8] Alison J. Farmer and E. Sterl Phinney, “The gravitational wave background from cosmological compact binaries,” *Mon. Not. Roy. Astron. Soc.* **346**, 1197 (2003), [arXiv:astro-ph/0304393](#).
- [9] Tania Regimbau, “The astrophysical gravitational wave stochastic background,” *Res. Astron. Astrophys.* **11**, 369–390 (2011), [arXiv:1101.2762 \[astro-ph.CO\]](#).
- [10] Xing-Jiang Zhu, E. Howell, T. Regimbau, D. Blair, and Zong-Hong Zhu, “Stochastic Gravitational Wave Background from Coalescing Binary Black Holes,” *Astrophys. J.* **739**, 86 (2011), [arXiv:1104.3565 \[gr-qc\]](#).
- [11] Tanmay Vachaspati and Alexander Vilenkin, “Gravitational Radiation from Cosmic Strings,” *Phys. Rev. D* **31**, 3052 (1985).

- [12] Arthur Kosowsky, Michael S. Turner, and Richard Watkins, “Gravitational waves from first order cosmological phase transitions,” *Phys. Rev. Lett.* **69**, 2026–2029 (1992).
- [13] M. C. Guzzetti, N. Bartolo, M. Liguori, and S. Matarrese, “Gravitational waves from inflation,” *Riv. Nuovo Cim.* **39**, 399–495 (2016), arXiv:1605.01615 [astro-ph.CO].
- [14] Chiara Caprini and Daniel G. Figueroa, “Cosmological Backgrounds of Gravitational Waves,” *Class. Quant. Grav.* **35**, 163001 (2018), arXiv:1801.04268 [astro-ph.CO].
- [15] Nancy Aggarwal *et al.*, “Challenges and opportunities of gravitational-wave searches at MHz to GHz frequencies,” *Living Rev. Rel.* **24**, 4 (2021), arXiv:2011.12414 [gr-qc].
- [16] Vasyly Alba and Juan Maldacena, “Primordial gravity wave background anisotropies,” *JHEP* **03**, 115 (2016), arXiv:1512.01531 [hep-th].
- [17] Jing Liu, Rong-Gen Cai, and Zong-Kuan Guo, “Large Anisotropies of the Stochastic Gravitational Wave Background from Cosmic Domain Walls,” *Phys. Rev. Lett.* **126**, 141303 (2021), arXiv:2010.03225 [astro-ph.CO].
- [18] Carlo R. Contaldi, “Anisotropies of Gravitational Wave Backgrounds: A Line Of Sight Approach,” *Phys. Lett. B* **771**, 9–12 (2017), arXiv:1609.08168 [astro-ph.CO].
- [19] Michael Geller, Anson Hook, Raman Sundrum, and Yuhsin Tsai, “Primordial Anisotropies in the Gravitational Wave Background from Cosmological Phase Transitions,” *Phys. Rev. Lett.* **121**, 201303 (2018), arXiv:1803.10780 [hep-ph].
- [20] N. Bartolo, D. Bertacca, S. Matarrese, M. Peloso, A. Ricciardone, A. Riotto, and G. Tasinato, “Anisotropies and non-Gaussianity of the Cosmological Gravitational Wave Background,” *Phys. Rev. D* **100**, 121501 (2019), arXiv:1908.00527 [astro-ph.CO].
- [21] Nicola Bartolo, Daniele Bertacca, Sabino Matarrese, Marco Peloso, Angelo Ricciardone, Antonio Riotto, and Gianmassimo Tasinato, “Characterizing the cosmological gravitational wave background: Anisotropies and non-Gaussianity,” *Phys. Rev. D* **102**, 023527 (2020), arXiv:1912.09433 [astro-ph.CO].
- [22] L. Valbusa Dall’Armi, A. Ricciardone, Nicola Bartolo, D. Bertacca, and S. Matarrese, “Imprint of relativistic particles on the anisotropies of the stochastic gravitational-wave background,” *Phys. Rev. D* **103**, 023522 (2021), arXiv:2007.01215 [astro-ph.CO].
- [23] Yongping Li, Fa Peng Huang, Xiao Wang, and Xinmin Zhang, “Anisotropy of phase transition gravitational wave and its implication for primordial seeds of the Universe,” *Phys. Rev. D* **105**, 083527 (2022), arXiv:2112.01409 [astro-ph.CO].
- [24] Florian Schulze, Lorenzo Valbusa Dall’Armi, Julien Lesgourgues, Angelo Ricciardone, Nicola Bartolo, Daniele Bertacca, Christian Fidler, and Sabino Matarrese, “GW_CLASS: Cosmological Gravitational Wave Background in the Cosmic Linear Anisotropy Solving System,” (2023), arXiv:2305.01602 [gr-qc].
- [25] Yanou Cui, Soubhik Kumar, Raman Sundrum, and Yuhsin Tsai, “Unraveling Cosmological Anisotropies within Stochastic Gravitational Wave Backgrounds,” (2023), arXiv:2307.10360 [astro-ph.CO].
- [26] Sai Wang, Zhi-Chao Zhao, Jun-Peng Li, and Qing-Hua Zhu, “Implications of Pulsar Timing Array Data for Scalar-Induced Gravitational Waves and Primordial Black Holes: Primordial Non-Gaussianity f_{NL} Considered,” (2023), arXiv:2307.00572 [astro-ph.CO].
- [27] Jun-Peng Li, Sai Wang, Zhi-Chao Zhao, and Kazunori Kohri, “Primordial Non-Gaussianity f_{NL} and Anisotropies in Scalar-Induced Gravitational Waves,” (2023), arXiv:2305.19950 [astro-ph.CO].
- [28] L. Valbusa Dall’Armi, A. Nishizawa, A. Ricciardone, and S. Matarrese, “Circular Polarization of the Astrophysical Gravitational Wave Background,” *Phys. Rev. Lett.* **131**, 041401 (2023), arXiv:2301.08205 [astro-ph.CO].
- [29] Laura Bethke, Daniel G. Figueroa, and Arttu Rajantie, “Anisotropies in the Gravitational Wave Background from Preheating,” *Phys. Rev. Lett.* **111**, 011301 (2013), arXiv:1304.2657 [astro-ph.CO].
- [30] Giulia Cusin, Cyril Pitrou, and Jean-Philippe Uzan, “Anisotropy of the astrophysical gravitational wave background: Analytic expression of the angular power spectrum and correlation with cosmological observations,” *Phys. Rev. D* **96**, 103019 (2017), arXiv:1704.06184 [astro-ph.CO].
- [31] Giulia Cusin, Irina Dvorkin, Cyril Pitrou, and Jean-Philippe Uzan, “First predictions of the angular power spectrum of the astrophysical gravitational wave background,” *Phys. Rev. Lett.* **120**, 231101 (2018), arXiv:1803.03236 [astro-ph.CO].
- [32] Alexander C. Jenkins, Richard O’Shaughnessy, Mairi Sakellariadou, and Daniel Wysocki, “Anisotropies in the astrophysical gravitational-wave background: The impact of black hole distributions,” *Phys. Rev. Lett.* **122**, 111101 (2019), arXiv:1810.13435 [astro-ph.CO].
- [33] Giulia Cusin, Irina Dvorkin, Cyril Pitrou, and Jean-Philippe Uzan, “Properties of the stochastic astrophysical gravitational wave background: astrophysical sources dependencies,” *Phys. Rev. D* **100**, 063004 (2019), arXiv:1904.07797 [astro-ph.CO].
- [34] Daniele Bertacca, Angelo Ricciardone, Nicola Bellomo, Alexander C. Jenkins, Sabino Matarrese, Alvise Raccanelli, Tania Regimbau, and Mairi Sakellariadou, “Projection effects on the observed angular spectrum of the astrophysical stochastic gravitational wave background,” *Phys. Rev. D* **101**, 103513 (2020), arXiv:1909.11627 [astro-ph.CO].
- [35] Nicola Bellomo, Daniele Bertacca, Alexander C. Jenkins, Sabino Matarrese, Alvise Raccanelli, Tania Regimbau, Angelo Ricciardone, and Mairi Sakellariadou, “CLASS_GWB: robust modeling of the astrophysical gravitational wave background anisotropies,” *JCAP* **06**, 030 (2022), arXiv:2110.15059 [gr-qc].
- [36] Gabriela Sato-Polito and Marc Kamionkowski, “Exploring the spectrum of stochastic gravitational-wave anisotropies with pulsar timing arrays,” (2023), arXiv:2305.05690 [astro-ph.CO].
- [37] Nihan Pol, Stephen R. Taylor, and Joseph D. Romano, “Forecasting Pulsar Timing Array Sensitivity to Anisotropy in the Stochastic Gravitational Wave Background,” *Astrophys. J.* **940**, 173 (2022), arXiv:2206.09936 [astro-ph.HE].
- [38] Yan-Heng Yu and Sai Wang, “Anisotropies in scalar-induced gravitational-wave background from inflaton-curvaton mixed scenario with sound speed resonance,” *Phys. Rev. D* **109**, 083501 (2024), arXiv:2310.14606 [astro-ph.CO].
- [39] David Alonso, Giulia Cusin, Pedro G. Ferreira, and

- Cyril Pitrou, “Detecting the anisotropic astrophysical gravitational wave background in the presence of shot noise through cross-correlations,” *Phys. Rev. D* **102**, 023002 (2020), [arXiv:2002.02888 \[astro-ph.CO\]](#).
- [40] David Alonso, Carlo R. Contaldi, Giulia Cusin, Pedro G. Ferreira, and Arianna I. Renzini, “Noise angular power spectrum of gravitational wave background experiments,” *Phys. Rev. D* **101**, 124048 (2020), [arXiv:2005.03001 \[astro-ph.CO\]](#).
- [41] Angelo Ricciardone, Lorenzo Valbusa Dall’Armi, Nicola Bartolo, Daniele Bertacca, Michele Liguori, and Sabino Matarrese, “Cross-Correlating Astrophysical and Cosmological Gravitational Wave Backgrounds with the Cosmic Microwave Background,” *Phys. Rev. Lett.* **127**, 271301 (2021), [arXiv:2106.02591 \[astro-ph.CO\]](#).
- [42] Giulia Capurri, Andrea Lapi, and Carlo Baccigalupi, “Detectability of the Cross-Correlation between CMB Lensing and Stochastic GW Background from Compact Object Mergers,” *Universe* **8**, 160 (2022), [arXiv:2111.04757 \[astro-ph.CO\]](#).
- [43] Alexander C. Jenkins, Mairi Sakellariadou, Tania Regimbau, and Eric Slezak, “Anisotropies in the astrophysical gravitational-wave background: Predictions for the detection of compact binaries by LIGO and Virgo,” *Phys. Rev. D* **98**, 063501 (2018), [arXiv:1806.01718 \[astro-ph.CO\]](#).
- [44] Zhi-Chao Zhao and Sai Wang, “Measuring the anisotropies in astrophysical and cosmological gravitational-wave backgrounds with Taiji and LISA networks,” *Sci. China Phys. Mech. Astron.* **67**, 120411 (2024), [arXiv:2407.09380 \[gr-qc\]](#).
- [45] Giulia Capurri, Andrea Lapi, Lumen Boco, and Carlo Baccigalupi, “Searching for Anisotropic Stochastic Gravitational-wave Backgrounds with Constellations of Space-based Interferometers,” *Astrophys. J.* **943**, 72 (2023), [arXiv:2212.06162 \[gr-qc\]](#).
- [46] A. I. Renzini and C. R. Contaldi, “Mapping Incoherent Gravitational Wave Backgrounds,” *Mon. Not. Roy. Astron. Soc.* **481**, 4650–4661 (2018), [arXiv:1806.11360 \[astro-ph.IM\]](#).
- [47] Arianna Renzini and Carlo Contaldi, “Improved limits on a stochastic gravitational-wave background and its anisotropies from Advanced LIGO O1 and O2 runs,” *Phys. Rev. D* **100**, 063527 (2019), [arXiv:1907.10329 \[gr-qc\]](#).
- [48] Sharan Banagiri, Alexander Criswell, Tommy Kuan, Vuk Mandic, Joseph D Romano, and Stephen R Taylor, “Mapping the gravitational-wave sky with lisa: a bayesian spherical harmonic approach,” *Monthly Notices of the Royal Astronomical Society* **507**, 5451–5462 (2021).
- [49] Nicola Bartolo *et al.* (LISA Cosmology Working Group), “Probing anisotropies of the Stochastic Gravitational Wave Background with LISA,” *JCAP* **11**, 009 (2022), [arXiv:2201.08782 \[astro-ph.CO\]](#).
- [50] Adrian Ka-Wai Chung and Nicolas Yunes, “Untargeted Bayesian search of anisotropic gravitational-wave backgrounds through the analytical marginalization of the posterior,” *Phys. Rev. D* **108**, 043032 (2023), [arXiv:2305.06502 \[gr-qc\]](#).
- [51] Leo Tsukada, Santiago Jaraba, Deepali Agarwal, and Erik Floden, “Bayesian parameter estimation for targeted anisotropic gravitational-wave background,” *Phys. Rev. D* **107**, 023024 (2023), [arXiv:2208.14421 \[astro-ph.IM\]](#).
- [52] Jonathan Gair, Joseph D. Romano, Stephen Taylor, and Chiara M. F. Mingarelli, “Mapping gravitational-wave backgrounds using methods from CMB analysis: Application to pulsar timing arrays,” *Phys. Rev. D* **90**, 082001 (2014), [arXiv:1406.4664 \[gr-qc\]](#).
- [53] Zhi-Yuan Li, Zheng-Cheng Liang, En-Kun Li, Jiandong Zhang, and Yi-Ming Hu, “Mapping Anisotropies in the Stochastic Gravitational-Wave Background with TianQin,” (2024), [arXiv:2409.11245 \[gr-qc\]](#).
- [54] Ran Ding and Chi Tian, “On the anisotropies of the cosmological gravitational-wave background from pulsar timing array observations,” *JCAP* **02**, 016 (2024), [arXiv:2309.01643 \[astro-ph.CO\]](#).
- [55] Kate Z. Yang, Jishnu Suresh, Giulia Cusin, Sharan Banagiri, Noelle Feist, Vuk Mandic, Claudia Scarlata, and Ioannis Michaloliakos, “Measurement of the cross-correlation angular power spectrum between the stochastic gravitational wave background and galaxy overdensity,” *Phys. Rev. D* **108**, 043025 (2023), [arXiv:2304.07621 \[gr-qc\]](#).
- [56] Pau Amaro-Seoane *et al.* (LISA), “Laser Interferometer Space Antenna,” (2017), [arXiv:1702.00786 \[astro-ph.IM\]](#).
- [57] K. G. Arun *et al.* (LISA), “New horizons for fundamental physics with LISA,” *Living Rev. Rel.* **25**, 4 (2022), [arXiv:2205.01597 \[gr-qc\]](#).
- [58] Tristan L. Smith, Tristan L. Smith, Robert R. Caldwell, and Robert Caldwell, “LISA for Cosmologists: Calculating the Signal-to-Noise Ratio for Stochastic and Deterministic Sources,” *Phys. Rev. D* **100**, 104055 (2019), [Erratum: *Phys.Rev.D* 105, 029902 (2022)], [arXiv:1908.00546 \[astro-ph.CO\]](#).
- [59] Rutger van Haasteren and Yuri Levin, “Understanding and analysing time-correlated stochastic signals in pulsar timing,” *Mon. Not. Roy. Astron. Soc.* **428**, 1147 (2013), [arXiv:1202.5932 \[astro-ph.IM\]](#).
- [60] Chiara Caprini, Ryusuke Jinno, Marek Lewicki, Eric Mudge, Marco Merchand, Germano Nardini, Mauro Pieroni, Alberto Roper Pol, and Ville Vaskonen (LISA Cosmology Working Group), “Gravitational waves from first-order phase transitions in LISA: reconstruction pipeline and physics interpretation,” *JCAP* **10**, 020 (2024), [arXiv:2403.03723 \[astro-ph.CO\]](#).
- [61] Nicola Bartolo *et al.*, “Science with the space-based interferometer LISA. IV: Probing inflation with gravitational waves,” *JCAP* **12**, 026 (2016), [arXiv:1610.06481 \[astro-ph.CO\]](#).
- [62] K. M. Górski, E. Hivon, A. J. Banday, B. D. Wandelt, F. K. Hansen, M. Reinecke, and M. Bartelman, “HEALPix - A Framework for high resolution discretization, and fast analysis of data distributed on the sphere,” *Astrophys. J.* **622**, 759–771 (2005), [arXiv:astro-ph/0409513](#).
- [63] Louis J. Rubbo, Neil J. Cornish, and Olivier Poujade, “Forward modeling of space borne gravitational wave detectors,” *Phys. Rev. D* **69**, 082003 (2004), [arXiv:gr-qc/0311069](#).
- [64] Reginald Christian Bernardo and Kin-Wang Ng, “Pulsar and cosmic variances of pulsar timing-array correlation measurements of the stochastic gravitational wave background,” *JCAP* **11**, 046 (2022), [arXiv:2209.14834 \[gr-qc\]](#).
- [65] Jun Luo *et al.* (TianQin), “TianQin: a space-borne

- gravitational wave detector,” *Class. Quant. Grav.* **33**, 035010 (2016), [arXiv:1512.02076 \[astro-ph.IM\]](#).
- [66] Wen-Rui Hu and Yue-Liang Wu, “The Taiji Program in Space for gravitational wave physics and the nature of gravity,” *Natl. Sci. Rev.* **4**, 685–686 (2017).
- [67] Wen-Hong Ruan, Zong-Kuan Guo, Rong-Gen Cai, and Yuan-Zhong Zhang, “Taiji program: Gravitational-wave sources,” *Int. J. Mod. Phys. A* **35**, 2050075 (2020), [arXiv:1807.09495 \[gr-qc\]](#).
- [68] Seiji Kawamura *et al.*, “The Japanese space gravitational wave antenna: DECIGO,” *Class. Quant. Grav.* **28**, 094011 (2011).
- [69] Michele Maggiore *et al.*, “Science Case for the Einstein Telescope,” *JCAP* **03**, 050 (2020), [arXiv:1912.02622 \[astro-ph.CO\]](#).
- [70] Alejandro Torres-Orjuela, Shun-Jia Huang, Zheng-Cheng Liang, Shuai Liu, Hai-Tian Wang, Chang-Qing Ye, Yi-Ming Hu, and Jianwei Mei, “Detection of astrophysical gravitational wave sources by TianQin and LISA,” *Sci. China Phys. Mech. Astron.* **67**, 259511 (2024), [arXiv:2307.16628 \[gr-qc\]](#).
- [71] Alejandro Torres-Orjuela, “Joint gravitational wave detection by TianQin and LISA,” in *7th International Workshop on the TianQin Science Mission* (2024) [arXiv:2407.11293 \[astro-ph.HE\]](#).
- [72] Zheng-Cheng Liang, Zhi-Yuan Li, En-Kun Li, Jian-dong Zhang, and Yi-Ming Hu, “Unveiling a multi-component stochastic gravitational-wave background with the TianQin + LISA network,” (2024), [arXiv:2409.00778 \[gr-qc\]](#).

Supplemental Material

I. Conditional probability distribution considering cross-correlation angular power spectrum

A multidimensional complex Gaussian distribution for d -dimensional variable \mathbf{x} is given by

$$\mathcal{N}(\boldsymbol{\mu}, \boldsymbol{\Sigma}) = \frac{1}{\pi^d |\boldsymbol{\Sigma}|} \exp [-(\mathbf{x} - \boldsymbol{\mu})^T \boldsymbol{\Sigma}^{-1} (\mathbf{x} - \boldsymbol{\mu})] . \quad (\text{S1})$$

Suppose that the vector $\mathbf{x} = [\mathbf{x}_1^T, \mathbf{x}_2^T]^T$ obeys joint gaussian distribution

$$p(\mathbf{x}) \sim \mathcal{N} \left(\begin{bmatrix} \boldsymbol{\mu}_1 \\ \boldsymbol{\mu}_2 \end{bmatrix}, \begin{bmatrix} \boldsymbol{\Sigma}_{11} & \boldsymbol{\Sigma}_{12} \\ \boldsymbol{\Sigma}_{12}^T & \boldsymbol{\Sigma}_{22} \end{bmatrix} \right), \quad (\text{S2})$$

where $\boldsymbol{\Sigma}_{12}$ is the non-symmetric cross-covariance matrix between \mathbf{x}_1 and \mathbf{x}_2 . Then the marginal distributions are

$$p(\mathbf{x}_1) = \int p(\mathbf{x}) d\mathbf{x}_2 \sim \mathcal{N}(\boldsymbol{\mu}_1, \boldsymbol{\Sigma}_{11}), \quad p(\mathbf{x}_2) = \int p(\mathbf{x}) d\mathbf{x}_1 \sim \mathcal{N}(\boldsymbol{\mu}_2, \boldsymbol{\Sigma}_{22}), \quad (\text{S3})$$

and according to the definition, the conditional probability distributions are

$$\begin{aligned} p(\mathbf{x}_1|\mathbf{x}_2) &\sim \mathcal{N} \left(\boldsymbol{\mu}_1 + \boldsymbol{\Sigma}_{12} \boldsymbol{\Sigma}_{22}^{-1} (\mathbf{x}_2 - \boldsymbol{\mu}_2), \boldsymbol{\Sigma}_{11} - \boldsymbol{\Sigma}_{12} \boldsymbol{\Sigma}_{22}^{-1} \boldsymbol{\Sigma}_{12}^T \right), \\ p(\mathbf{x}_2|\mathbf{x}_1) &\sim \mathcal{N} \left(\boldsymbol{\mu}_2 + \boldsymbol{\Sigma}_{12}^T \boldsymbol{\Sigma}_{11}^{-1} (\mathbf{x}_1 - \boldsymbol{\mu}_1), \boldsymbol{\Sigma}_{22} - \boldsymbol{\Sigma}_{12}^T \boldsymbol{\Sigma}_{11}^{-1} \boldsymbol{\Sigma}_{12} \right). \end{aligned} \quad (\text{S4})$$

We now apply the results above to construct the likelihood function, incorporating the cross-correlations between the GWB and any known cosmological tracers. Assuming that the GWB and a set of cosmological tracers \mathbf{Y} , characterized by spherical harmonic coefficients $a_{\ell m}^{\text{GW}}$ and $a_{\ell m}^{\mathbf{Y}}$ respectively, are multivariate Gaussian random variables with zero mean and covariance $C_\ell^{\text{GW} \times \mathbf{Y}}$. Following eq. (S2), their probability distribution is given by

$$p(a_{\{\ell m\}}^{\text{GW}}, a_{\{\ell m\}}^{\mathbf{Y}}) = \prod_{\ell=1}^{\ell_{\max}} \prod_{m=-\ell}^{\ell} \frac{\exp \left\{ - \begin{pmatrix} a_{\ell m}^{\text{GW}} \\ a_{\ell m}^{\mathbf{Y}} \end{pmatrix}^T \begin{pmatrix} C_\ell^{\text{GW}} & C_\ell^{\text{GW} \times \mathbf{Y}} \\ C_\ell^{\text{GW} \times \mathbf{Y}} & C_\ell^{\mathbf{Y}} \end{pmatrix}^{-1} \begin{pmatrix} a_{\ell m}^{\text{GW}} \\ a_{\ell m}^{\mathbf{Y}} \end{pmatrix} \right\}}{\pi \left(C_\ell^{\text{GW}} C_\ell^{\mathbf{Y}} - (C_\ell^{\text{GW} \times \mathbf{Y}})^2 \right)}. \quad (\text{S5})$$

According to eq. (S4), the conditional distribution of $a_{\ell m}^{\text{GW}}$ for given $a_{\ell m}^{\mathbf{Y}}$ obeys

$$p(a_{\{\ell m\}}^{\text{GW}} | a_{\{\ell m\}}^{\mathbf{Y}}, \mu_{\{\ell m\}}^{\text{GW}|\mathbf{Y}}, C_{\{\ell\}}^{\text{GW}|\mathbf{Y}}) = \prod_{\ell=1}^{\ell_{\max}} \prod_{m=-\ell}^{\ell} \frac{\exp \left\{ - \left(a_{\ell m}^{\text{GW}} - \mu_{\ell m}^{\text{GW}|\mathbf{Y}} \right) \left(C_\ell^{\text{GW}|\mathbf{Y}} \right)^{-1} \left(a_{\ell m}^{\text{GW}} - \mu_{\ell m}^{\text{GW}|\mathbf{Y}} \right) \right\}}{\pi C_\ell^{\text{GW}|\mathbf{Y}}}, \quad (\text{S6})$$

where the mean and the covariance are given by

$$\mu_{\ell m}^{\text{GW}|\mathbf{Y}} = \frac{C_{\ell}^{\text{GW} \times \mathbf{Y}}}{C_{\ell}^{\mathbf{Y}}} a_{\ell m}, \quad (\text{S7})$$

$$C_{\ell}^{\text{GW}|\mathbf{Y}} = C_{\ell}^{\text{GW}} - \frac{(C_{\ell}^{\text{GW} \times \mathbf{Y}})^2}{C_{\ell}^{\mathbf{Y}}} = C_{\ell}^{\text{GW}} \left[1 - \left(\frac{C_{\ell}^{\text{GW} \times \mathbf{Y}}}{\sqrt{C_{\ell}^{\text{GW}} C_{\ell}^{\mathbf{Y}}}} \right)^2 \right]. \quad (\text{S8})$$

From now on, for simplicity, we will focus on a single tracer, \mathbf{Y} , instead of a set of tracers, \mathbf{Y} , although the generalization to multiple tracers are straightforward. Using eq. (3), we obtain the likelihood for the GWB intensity

$$\begin{aligned} \mathcal{L}(I_{\{\ell m\},f} | \text{GW} \times \mathbf{Y}) &\equiv p(I_{\{\ell m\},f} | a_{\{\ell m\}}^{\mathbf{Y}}, \mu_{\{\ell m\}}^{\text{GW}|\mathbf{Y}}, C_{\{\ell\}}^{\text{GW}|\mathbf{Y}}) \\ &= \prod_{\ell=1}^{\ell_{\max}} \prod_{m=-\ell}^{\ell} \frac{\exp \left\{ - \left(I_{\ell m} - K_f \mu_{\ell m}^{\text{GW}|\mathbf{Y}} \right) \left(K_f^2 C_{\ell}^{\text{GW}|\mathbf{Y}} \right)^{-1} \left(I_{\ell m} - K_f \mu_{\ell m}^{\text{GW}|\mathbf{Y}} \right) \right\}}{\pi C_{\ell}^{\text{GW}|\mathbf{Y}}}. \end{aligned} \quad (\text{S9})$$

For the sake of conciseness, we introduce the following compact notations:

$$\begin{aligned} a &= \{AB\} = \underbrace{\{1, 1\}, \{1, 2\}, \dots, \{1, n\}, \dots, \{n, 1\}, \dots, \{n, n\}}_{n \times n \text{ terms}}, \\ \mu &= \{\ell m\} = \underbrace{\{1, -1\}, \{1, 0\}, \{1, 1\}, \dots, \{\ell_{\max}, -\ell_{\max}\}, \dots, \{\ell_{\max}, \ell_{\max}\}}_{\ell_{\max}(\ell_{\max}+2) \text{ terms}}, \\ \Gamma_{a0} &\equiv \gamma_{00}^{\{AB\}}, \quad \Gamma_{a\mu} \equiv \gamma_{\{\ell m\}}^{\{AB\}}, \quad X_0 = \bar{X}_0 \equiv I_{00}, \quad X_{\mu} \equiv I_{\{\ell m\}}, \quad \bar{X}_{\mu} \equiv K_f \mu_{\{\ell m\}}^{\text{GW}|\mathbf{Y}}, \\ D_a &\equiv D_{tf}^{AB}, \quad N_a \equiv N_f^{AB}, \quad S_a \equiv \langle D_{tf}^{AB} \rangle = \Gamma_{a0} X_0 + \Gamma_{a\mu} X_{\mu} + N_a, \quad (C_D)_{ab} \equiv C_{t,f}^{ABCD}, \\ (C_I)_{\mu\nu} &\equiv K_f^2 \text{diag} \left(\underbrace{C_1^{\text{GW}|\mathbf{Y}}, C_1^{\text{GW}|\mathbf{Y}}, C_1^{\text{GW}|\mathbf{Y}}, \dots, C_{\ell_{\max}}^{\text{GW}|\mathbf{Y}}, \dots, C_{\ell_{\max}}^{\text{GW}|\mathbf{Y}}}_{\ell_{\max}(\ell_{\max}+2) \text{ terms}} \right), \end{aligned} \quad (\text{S10})$$

for which the likelihood in eq. (8) and (S9) are written as

$$\mathcal{L}(D_{t,f} | I_{\{\ell m\},f}) = \frac{1}{|\pi C_D|} \exp \left\{ - \left(D_a - S_a \right)^{\dagger} (C_D)_{ab}^{-1} \left(D_b - S_b \right) \right\}, \quad (\text{S11})$$

$$\mathcal{L}(I_{\{\ell m\},f} | \text{GW} \times \mathbf{Y}) = \frac{1}{|\pi C_I|} \exp \left\{ - \left(X_{\mu} - \bar{X}_{\mu} \right)^{\dagger} (C_I)_{\mu\nu}^{-1} \left(X_{\nu} - \bar{X}_{\nu} \right) \right\}. \quad (\text{S12})$$

II. Likelihood function with marginalizations

The likelihood connecting the entire time-series data and the angular power spectrum can be obtained by marginalizing over $I_{\{\ell m\}}$ through

$$\begin{aligned} \mathcal{L}(D_{\{t,f\}} | \text{GW} \times \mathbf{Y}) &\propto \prod_{t,f} \int \mathcal{D}I_{\ell m,f} \mathcal{L}(D_{t,f} | I_{\{\ell m\},f}) \mathcal{L}(I_{\{\ell m\},f} | \text{GW} \times \mathbf{Y}) \\ &= \prod_{t,f} \frac{1}{|\pi C_D| |\pi C_I|} \int \left[\prod_{\ell=1}^{\ell_{\max}} \prod_{m=-\ell}^{\ell} d^2 X_{\rho} \right] \exp \left\{ - \left(D_a - \bar{X}_0 \Gamma_{0a} - X_{\mu} \Gamma_{\mu a} - N_a \right)^* (C_D)_{ab}^{-1} \right. \\ &\quad \left. \left(D_b - \Gamma_{b0} \bar{X}_0 - \Gamma_{b\nu} X_{\nu} - N_b \right) - \left(X_{\mu} - \bar{X}_{\mu} \right)^{\dagger} (C_I)_{\mu\nu}^{-1} \left(X_{\nu} - \bar{X}_{\nu} \right) \right\}, \end{aligned} \quad (\text{S13})$$

where $d^2 X_\rho = d\text{Re}X_\rho d\text{Im}X_\rho$, and the dimension of the integral is $d = \ell_{\max}(\ell_{\max} + 2)$. Utilizing the complex Gaussian integration formula

$$\int d^{2d} z \exp(-z^\dagger M z + K^\dagger z + z^\dagger K + Q) = \frac{\pi^d}{|M|} \exp(K^\dagger M^{-1} K + Q), \quad (\text{S14})$$

the likelihood eq. (S13) reads

$$\mathcal{L}(D_{\{t,f\}} | \text{GW} \times Y) = \prod_{t,f} \frac{1}{|\pi C_D| |C_I| |M|} \exp(K_\mu^\dagger M_{\mu\nu}^{-1} K_\nu + Q), \quad (\text{S15})$$

$$M_{\mu\nu}^{-1} = ((C_I)_{\mu\nu}^{-1} + \Gamma_{\mu a}^* (C_D)_{ab}^{-1} \Gamma_{b\nu})^{-1}, \quad (\text{S16})$$

$$K_\mu = \Gamma_{\mu a}^* (C_D)_{ab}^{-1} (D_b - \Gamma_{b0} \bar{X}_0 - N_b) + (C_I)_{\mu\nu}^{-1} \bar{X}_\nu, \quad (\text{S17})$$

$$Q = - (D_a - \bar{X}_0 \Gamma_{0a} - N_a)^* (C_D)_{ab}^{-1} (D_b - \Gamma_{b0} \bar{X}_0 - N_b) - \bar{X}_\mu^\dagger (C_I)_{\mu\nu}^{-1} \bar{X}_\nu. \quad (\text{S18})$$

We will show that eq. (S15) can be reformulated into a more concise expression, providing a clearer representation of the underlying physics. To see this, we employ Sherman-Morrison-Woodbury matrix inversion lemma, written as

$$(A + X B X^\dagger)^{-1} = A^{-1} - A^{-1} X (B^{-1} + X^\dagger A^{-1} X)^{-1} X^\dagger A^{-1}, \quad (\text{S19})$$

$$|A + X B X^\dagger| = |B| |A| |B^{-1} + X^\dagger A^{-1} X|, \quad (\text{S20})$$

where A and B are square and invertible matrices, though not necessarily of the same dimension. From which, adopting the matrix form, we obtain following relations:

$$\begin{aligned} (C_D + \Gamma C_I \Gamma^\dagger)^{-1} &= C_D^{-1} - C_D^{-1} \Gamma (C_I^{-1} + \Gamma^\dagger C_D^{-1} \Gamma)^{-1} \Gamma^\dagger C_D^{-1} \\ &\simeq C_D^{-1} - C_D^{-1} \Gamma C_I \Gamma^\dagger C_D^{-1}, \end{aligned} \quad (\text{S21})$$

$$\begin{aligned} (C_I^{-1} + \Gamma^\dagger C_D^{-1} \Gamma)^{-1} &= C_I - C_I \Gamma^\dagger (C_D + \Gamma C_I \Gamma^\dagger)^{-1} \Gamma C_I \\ &\simeq C_I - C_I \Gamma^\dagger C_D^{-1} \Gamma C_I, \end{aligned} \quad (\text{S22})$$

$$\begin{aligned} |C_D| |C_I| |M| &= |C_D| |C_I| |C_I^{-1} + \Gamma^\dagger C_D^{-1} \Gamma| \\ &= |C_D + \Gamma C_I \Gamma^\dagger|. \end{aligned} \quad (\text{S23})$$

The exponential term in eq. (S15) can be rearranged to get

$$\begin{aligned} &K_\mu^\dagger M_{\mu\nu}^{-1} K_\nu + Q \\ &= [(D_a - \Gamma \bar{X}_0 - N_a)^\dagger C_D^{-1} \Gamma + \bar{X}^\dagger C_I^{-1}] (C_I^{-1} + \Gamma^\dagger C_D^{-1} \Gamma)^{-1} [\Gamma^\dagger C_D^{-1} (D_b - \Gamma \bar{X}_0 - N_b) + C_I^{-1} \bar{X}] \\ &\quad - (D_a - \Gamma \bar{X}_0 - N_a)^\dagger C_D^{-1} (D_b - \Gamma \bar{X}_0 - N_b) - \bar{X}^\dagger C_I^{-1} \bar{X} \\ &= - (D_a - \Gamma \bar{X}_0 - N_a)^\dagger [C_D^{-1} - C_D^{-1} \Gamma (C_I^{-1} + \Gamma^\dagger C_D^{-1} \Gamma)^{-1} \Gamma^\dagger C_D^{-1}] (D_b - \Gamma \bar{X}_0 - N_b) \\ &\quad + (D_a - \Gamma \bar{X}_0 - N_a)^\dagger C_D^{-1} \Gamma (C_I^{-1} + \Gamma^\dagger C_D^{-1} \Gamma)^{-1} C_I^{-1} \bar{X} \\ &\quad + \bar{X}^\dagger C_I^{-1} (C_I^{-1} + \Gamma^\dagger C_D^{-1} \Gamma)^{-1} \Gamma^\dagger C_D^{-1} (D_b - \Gamma \bar{X}_0 - N_b) \\ &\quad + \bar{X}^\dagger C_I^{-1} (C_I^{-1} + \Gamma^\dagger C_D^{-1} \Gamma)^{-1} C_I^{-1} \bar{X} - \bar{X}^\dagger C_I^{-1} \bar{X} \\ &\simeq - (D_a - \Gamma \bar{X}_0 - N_a)^\dagger (C_D + \Gamma C_I \Gamma^\dagger)^{-1} (D_b - \Gamma \bar{X}_0 - N_b) \\ &\quad + (D_a - \Gamma \bar{X}_0 - N_a)^\dagger (C_D + \Gamma C_I \Gamma^\dagger)^{-1} \Gamma \bar{X} \\ &\quad + \bar{X}^\dagger \Gamma^\dagger (C_D + \Gamma C_I \Gamma^\dagger)^{-1} (D_b - \Gamma \bar{X}_0 - N_b) \\ &\quad - \bar{X}^\dagger \Gamma^\dagger (C_D + \Gamma C_I \Gamma^\dagger)^{-1} \Gamma \bar{X} \\ &= - (D_a - \Gamma \bar{X}_0 - N_a - \Gamma \bar{X})^\dagger (C_D + \Gamma C_I \Gamma^\dagger)^{-1} (D_b - \Gamma \bar{X}_0 - N_b - \Gamma \bar{X}). \end{aligned} \quad (\text{S24})$$

Taking into account the determinants, eq. (S15) then becomes

$$\begin{aligned} &\mathcal{L}(D_{\{t,f\}} | \text{GW} \times Y) \\ &= \prod_{t,f} \frac{1}{|\pi(C_D + \Gamma C_I \Gamma^\dagger)|} \exp \left\{ - (D_a - \Gamma \bar{X}_0 - N_a - \Gamma \bar{X})^\dagger (C_D + \Gamma C_I \Gamma^\dagger)^{-1} (D_b - \Gamma \bar{X}_0 - N_b - \Gamma \bar{X}) \right\}. \end{aligned} \quad (\text{S25})$$

Finally, to combine two terms associated with \bar{X} , we define $\bar{Z}_\mu \equiv \bar{X}_\mu$ for $\mu \geq 1$ and $\bar{Z}_0 \equiv \bar{X}_0$ for $\mu = 0$, and redefine

$$(C_I)_{\mu\nu} \equiv K_f^2 \text{diag} \left(\underbrace{0, C_1^{\text{GW|Y}}, C_1^{\text{GW|Y}}, C_1^{\text{GW|Y}}, \dots, C_{\ell_{\max}}^{\text{GW|Y}}, \dots, C_{\ell_{\max}}^{\text{GW|Y}}}_{(\ell_{\max}+1)^2 \text{ terms}}, \overbrace{\phantom{C_1^{\text{GW|Y}}, \dots, C_{\ell_{\max}}^{\text{GW|Y}}}}^{(2\ell_{\max}+1) \text{ terms}} \right), \quad (\text{S26})$$

to match the matrix dimensions, arriving the likelihood function in eq. (13)

$$\mathcal{L}(D_{\{t,f\}} | \text{GW} \times \text{Y}) \propto \prod_{t,f} |\pi C_{ab}|^{-1} \exp(-J_a^\dagger C_{ab}^{-1} J_b), \quad (\text{S27})$$

$$C_{ab} = C_{ab}^D + \Gamma_{a\mu} C_{\mu\nu}^I \Gamma_{\nu b}^*, \quad (\text{S28})$$

$$J_a = D_a - \Gamma_{a\mu} \bar{Z}_\mu - N_a. \quad (\text{S29})$$